International Journal of Modern Physics B
Vol. 30, No. 13 (2016) 1642008 (9 pages)

DOI: 10.1142/S021797921642008X

World Scientific
www.worldscientific.com

Energy spectrum and wavefunction of electrons in hybrid superconducting nanowires

S. P. Kruchinin

Bogolyubov Institute for Theoretical Physics,
National Academy of Sciences of Ukraine,
Kiev 03680, Ukraine
skruchin@i.com.ua

Accepted 29 February 2016
Published 28 March 2016

Recent experiments have fabricated structured arrays. We study hybrid nanowires, in which normal and superconducting regions are in close proximity, by using the Bogoliubov–de Gennes equations for superconductivity in a cylindrical nanowire. We succeed to obtain the quantum energy levels and wavefunctions of a superconducting nanowire. The obtained spectra of electrons remind Hofstadter's butterfly.

Keywords: Nanowires; Andreev state; energy spectrum; Hofstadter's butterfly.

PACS number: 74.20.-z

1. Introduction

Recent advances in nanoscience have demonstrated that the fundamentally new physical phenomena can be found, when, systems are reduced in size to dimensions, which become comparable to the fundamental microscopic length scales of the investigated material. Superconductivity is a macroscopic quantum phenomena, and, therefore, it is especially interesting to see how this quantum state is influenced when the samples are reduced to nanometer sizes. In such systems, new states of matter can be engineered that do not occur in bulk materials. A good example is the case of nanostructures composed of both superconducting and ferromagnetic metals. Here, the proximity effects couple the Cooper pair condensate to the spin-polarized band structure of the ferromagnet, allowing the local coexistence of both pairing and magnetism. In the bulk, the possibility of such coexistence was examined by Larkin–Ovchinnikov[1] and Fulde–Ferrell,[2] giving the so-called LOFF state. But it was proved difficult to find this state in bulk materials, possibly because of its high sensitivity to a disorder.[3,4]

In this paper, we consider composite nanowires made from both superconducting and ferromagnetic metals. We consider the cylindrical geometry shown in Fig. 1,

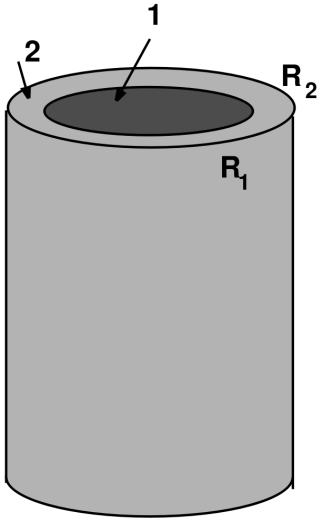

Fig. 1. Nanowire.

in which one metal forms the core of the nanowire and the second forms an outer cylindrical sheath. Mesoscopic wires with a similar geometry have been examined by Mota and coworkers.[5–9] In the case of a ferromagnetic core, we can compare the spectrum with results for planar hybrid S/F nanostructures, as reviewed recently by Lyuksyutov and Pokrovsky[10] and by Buzdin.[11] We mention the recent work on the superconductivity of ferromagnetic wires by Wang *et al.*[12] which presents the significant results on the anomalous effect of proximity revealed in superconducting magnetic wires. We also emphasize the promising direction in the fabrication of MgB_2 nanowires.[13]

Below, we will calculate the wavefunctions and the energy spectrum of electrons in hybrid superconducting nanowires. The spectrum of electrons reminds a fractal structure such as Hofstadter's butterfly introduced in 1976 for the description of a behavior of electrons in a magnetic field.[14]

2. Methodology

We model the hybrid superconductor–ferromagnet nanowire system by extending the self-consistent theory of a type II vortex developed by Gygi and Schlüter[15] to the case of a ferromagnetic vortex core. We start with the effective Pauli Hamiltonian for the spin-polarized electronic states of a normal metal:

$$\hat{H}^0_{\sigma\sigma'} = \frac{(\hat{p} + e\mathbf{A})^2}{2m_e}\delta_{\sigma\sigma'} + V_{\sigma\sigma'}(\mathbf{r})\,, \tag{1}$$

where $-e$ is the electron charge, $\mathbf{A}(\mathbf{r})$ is the magnetic vector potential, and $V_\sigma(\mathbf{r})$ is a general spin-dependent single potential, where σ is $\uparrow/\downarrow$. This potential can be assumed to be the sum of the ionic, Hartree and exchange-correlation potentials of

a self-consistent spin-polarized DFT calculation. In this case, it has the form:

$$V_\sigma(\mathbf{r}) = V_{\text{ion}}(\mathbf{r}) + V_H(\mathbf{r}) + V_{xc}(\mathbf{r}) + \mu_{\text{B}}(\mathbf{B} + \mathbf{B}_{xc})\sigma_{\sigma\sigma'}\,, \tag{2}$$

where $V_{xc}(\mathbf{r})$ is the spin-independent part of the exchange-correlation potential, μ_{B} is the Bohr magneton, $\mathbf{B}(\mathbf{r})$ is the physical local magnetic field and $\mathbf{B}_{xc}$ is an effective magnetic field representing the exchange field of spin-polarization in the ferromagnet. Here, $\sigma_{\sigma\sigma'}$ is the vector of Pauli matrices.

To model the superconducting elements of the hybrid system, this single-particle Hamiltonian is supplemented by an effective attraction, which we take as the BCS contact term

$$V(\mathbf{r}, \mathbf{r}') = -g(\mathbf{r})\delta(\mathbf{r} - \mathbf{r}')\,, \tag{3}$$

where $g(\mathbf{r})$ is the local attractive potential strength at $\mathbf{r}$. This will be zero in the normal or ferromagnetic part of the nanowire and a constant g in the superconducting parts. For simplicity, we neglect a retardation of the attraction in the rest of this paper.

The full effective Hamiltonian for our system is

$$\hat{H} = \int d^3r \left[\sum_{\sigma\sigma'}(\hat{\psi}^+_\sigma(\mathbf{r})\hat{H}^0_{\sigma\sigma'}\hat{\psi}_{\sigma'}(\mathbf{r})) - g(\mathbf{r})\hat{\psi}^+_\uparrow(\mathbf{r})\hat{\psi}^+_\downarrow(\mathbf{r})\hat{\psi}_\downarrow(\mathbf{r})\hat{\psi}_\uparrow(\mathbf{r})\right]. \tag{4}$$

Here, $\hat{\psi}^+_\sigma(\mathbf{r})$ and $\hat{\psi}_\sigma(\mathbf{r})$ are the usual field operators for the electrons. In the Hartree–Fock–Gorkov approximation, this Hamiltonian is diagonalized by a spin-dependent Bogoliubov–Valatin transformation

$$\hat{\psi}_\sigma(\mathbf{r}) = \sum_n (u_{n\sigma}(\mathbf{r})\hat{\gamma}_n + v^*_{n\sigma}(\mathbf{r})\hat{\gamma}^+_n)\,, \tag{5}$$

$$\hat{\psi}^+_\sigma(\mathbf{r}) = \sum_n (u^*_{n\sigma}(\mathbf{r})\hat{\gamma}^+_n + v_{n\sigma}(\mathbf{r})\hat{\gamma}_n)\,. \tag{6}$$

The requirement that the quasiparticle creation and annihilation operators retain the fermion anticommutation laws,

$$\{\hat{\gamma}_n, \hat{\gamma}^+_{n'}\} = \delta_{nn'}\,, \tag{7}$$

implies that

$$\sum_{n\sigma}(u^*_{n\sigma}(\mathbf{r})u_{n\sigma'}(\mathbf{r}') + v_{n\sigma}(\mathbf{r})v^*_{n\sigma'}(\mathbf{r}')) = \delta(\mathbf{r} - \mathbf{r}')\delta_{\sigma\sigma'}\,. \tag{8}$$

The resulting set of Bogoliubov–de Gennes equations is

$$\begin{pmatrix} \hat{H}_1 + V_{\uparrow\uparrow} & V_{\uparrow\downarrow} & 0 & \Delta(\mathbf{r}) \\ V_{\downarrow\uparrow} & \hat{H}_1 + V_{\downarrow\downarrow} & -\Delta(\mathbf{r}) & 0 \\ 0 & -\Delta^*(\mathbf{r}) & -\hat{H}_1 - V_{\uparrow\uparrow} & -V_{\uparrow\downarrow} \\ \Delta^*(\mathbf{r}) & 0 & -V_{\downarrow\uparrow} & -\hat{H}_1 - V_{\downarrow\downarrow} \end{pmatrix} \begin{pmatrix} u_{n\uparrow\sigma} \\ u_{n\downarrow\sigma} \\ v_{n\uparrow\sigma} \\ v_{n\downarrow\sigma} \end{pmatrix} = E_{n\sigma} \begin{pmatrix} u_{n\uparrow\sigma} \\ u_{n\downarrow\sigma} \\ v_{n\uparrow\sigma} \\ v_{n\downarrow\sigma} \end{pmatrix}, \tag{9}$$

where $\hat{H}_1 = (\hat{p} + e\mathbf{A})^2/2m_e - \mu$ and μ is the chemical potential.

The self-consistent pairing potential corresponds to a pure spin-singlet pairing state and is given by

$$\Delta(\mathbf{r}) = g\langle\hat{\psi}_{\uparrow}(\mathbf{r})\hat{\psi}_{\downarrow}(\mathbf{r})\rangle\,. \tag{10}$$

Consider the special case where the magnetization of the ferromagnet is in the same collinear direction, $\mathbf{B}_{xc}$, as the external field $\mathbf{B}$. Choosing it as the spin-quantization axis $\hat{z}$, we have $V_{\uparrow\downarrow} = V_{\downarrow\downarrow} = 0$. In this case, the full system of four matrix Bogoliubov–de Gennes equations is separated into a pair of 2×2 matrix equations

$$\begin{pmatrix} \hat{H}_1 + V_{\uparrow\uparrow} & \Delta(\mathbf{r}) \\ \Delta^*(\mathbf{r}) & -\hat{H}_1 - V_{\downarrow\downarrow} \end{pmatrix} \begin{pmatrix} u_{n\uparrow\sigma} \\ v_{n\downarrow\sigma} \end{pmatrix} = E_{n\sigma} \begin{pmatrix} u_{n\uparrow\sigma} \\ v_{n\downarrow\sigma} \end{pmatrix}, \tag{11}$$

$$\begin{pmatrix} \hat{H}_1 + V_{\downarrow\downarrow} & -\Delta(\mathbf{r}) \\ -\Delta^*(\mathbf{r}) & -\hat{H}_1 - V_{\uparrow\uparrow} \end{pmatrix} \begin{pmatrix} u_{n\downarrow\sigma} \\ v_{n\uparrow\sigma} \end{pmatrix} = E_{n\sigma} \begin{pmatrix} u_{n\downarrow\sigma} \\ v_{n\uparrow\sigma} \end{pmatrix}. \tag{12}$$

3. Calculation of the Spectrum

We will study the Bogoliubov–de Gennes equations, by using a numerical method for their solution. The calculation algorithm is realized with the use of the most powerful FORTRAN language specially developed for mathematical calculations.

In view of the cylindrical symmetry of the system under study, we write the system of Bogoliubov–de Gennes equations in the form suitable for calculations. We will also use the fact that the amplitudes of the functions $u(r)$ and $v(r)$ tend to zero at the boundary point. The solutions of the equations are determined with the use of the Runge–Kutta method.

Taking the symmetry of our system (cylindrical) into account and choosing the gauge, in which the parameter $\Delta(r)$ is real, we can write the system of Bogoliubov–de Gennes equations in the form:

$$\begin{aligned} \bar{u}(r,\theta,z) &= u_{\mu n k_z}(r) e^{-i\mu\theta} e^{-ik_z z}\,, \\ \bar{v}(r,\theta,z) &= v_{\mu n k_z}(r) e^{i\mu\theta} e^{-ik_z z}\,, \end{aligned} \tag{13}$$

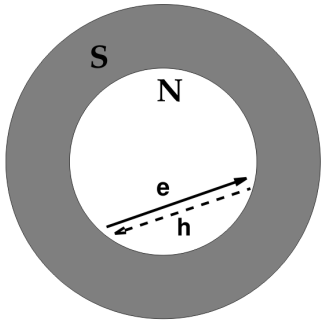

Fig. 2. Billiard 1.

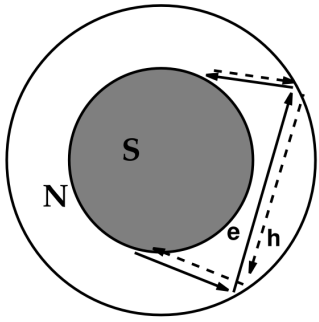

Fig. 3. Billiard 2.

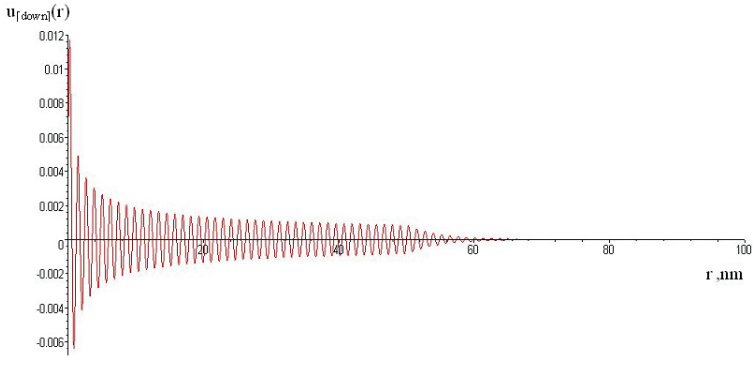

Fig. 4. Quasiparticle amplitude of the Andreev state.

$$
\begin{aligned}
-\frac{\partial^2}{\partial r^2}u_{\mu nk_z}(r) - \frac{1}{r}\frac{\partial}{\partial r}u_{\mu nk_z}(r) + U(r)\cdot u_{\mu nk_z}(r) + \Delta(r)\cdot v_{\mu nk_z}(r) = 0\,,\\
-\frac{\partial^2}{\partial r^2}v_{\mu nk_z}(r) - \frac{1}{r}\frac{\partial}{\partial r}v_{\mu nk_z}(r) + U(r)\cdot v_{\mu nk_z}(r) - \Delta(r)\cdot u_{\mu nk_z}(r) = 0\,,
\end{aligned}
\tag{14}
$$

where $U(r) = \mu^2/r^2 - (E_f - (k_z^2/m_z) - E_{\mu nk_z})$. The plot of wavefunctions is given in Fig. 4 ($E_0 = 0.986669921875$ eV, $E_f = 1$ eV, $\Delta = 0.1$ eV, $k_z = 0$, $R_1 = 50$ nm, $R_2 = 100$ nm and $\mu = 1$). In Figs. 5 and 6, we present the results of calculations for the spectrum of Andreev states of the system.

The resulting spectrum as a function of the angular momentum is shown in billiard 1 (Fig. 2) and billiard 2 (Fig. 3). The spectra demonstrate the splitting caused by the boundary effect.

4. Discussion

The Andreev billiard systems are the analog of a classical billiard. The Andreev billiard is interpreted as a ballistic motion with the Andreev reflection at the interface with a superconductor. The Andreev reflection is a fundamental process

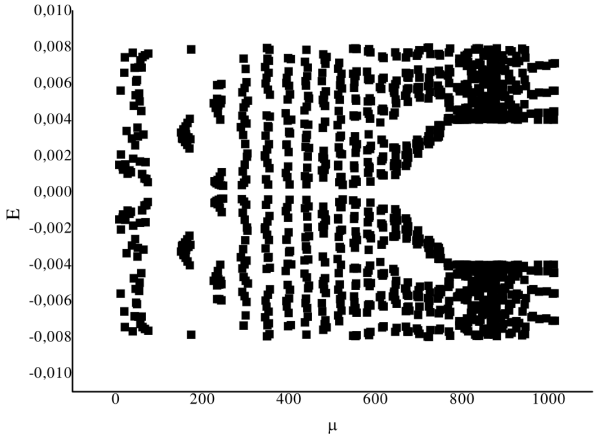

Fig. 5. Andreev spectrum as a function of the angular momentum for billiard 1.

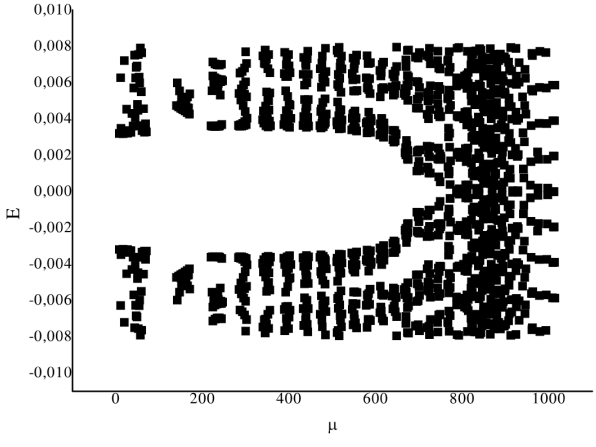

Fig. 6. Andreev spectrum as a function of the angular momentum for billiard 2.

that converts an electron incident on a superconductor into a hole, while a Cooper pair is added to the superconductivity condensate. Figures 5 and 6 demonstrate the electron–hole symmetry of the Andreev spectrum. One-dimensional solutions of the Bogoliubov–de Gennes equations pass into two-dimensional ones, as μ increases. It is worth noting that we work in the clean limit (mean free path $l \gg \lambda, \xi$).

Estimates of the penetration depth and the length scale of order were performed in Ref. 16:

$$\begin{cases} \lambda(T) = \dfrac{\lambda_0}{\sqrt{1-t^4}} \quad \text{where} \quad t = \dfrac{T}{T_c}\,, \\ \xi(T) = \dfrac{\xi_0(1-0.25t)}{\sqrt{1-t}}\,, \end{cases} \tag{15}$$

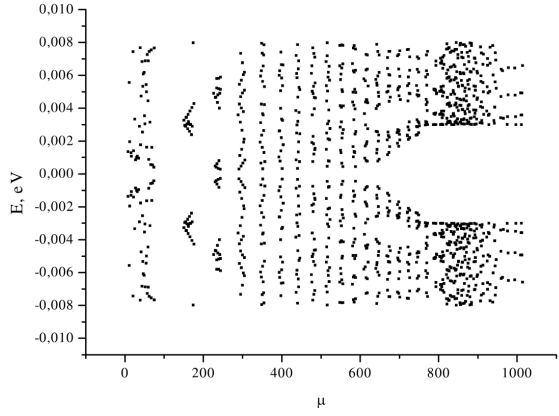

Fig. 7. Andreev spectrum for MgB_2 nanowires.

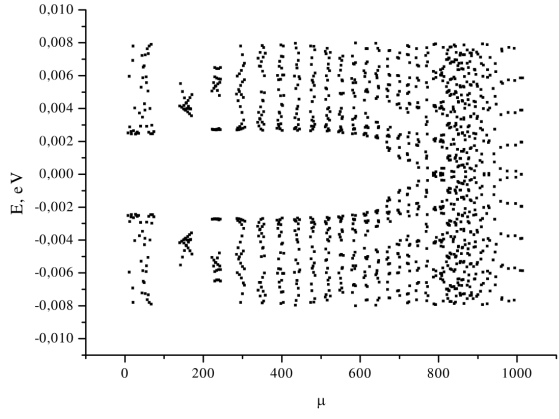

Fig. 8. Andreev spectrum for MgB_2 nanowires (SN).

where $\lambda_0 = 46$ nm and $\xi_0 = 74$ nm, i.e., almost the characteristic lengths of lead at zero temperature in the clean limit. We have carried out also the calculations for MgB_2 nanowires with the parameters namely $R_1 = 150$ nm, $R_2 = 200$ nm, $M_z = 0$, $k_z = 0$, $\Delta = 0.003$ eV and $E_f = 1$ eV. In Fig. 7 (NS, $R_1 = 150$ nm, $R_2 = 200$ nm, $M_z = 0$, $k_z = 0$, $\Delta = 0.003$ eV and $E_f = 1$ eV), we present the spectrum as a function of the angular momentum for MgB_2 nanowires Fig. 8 (billiard 2), whereas Fig. 9 shows the analogous dependence in the case of billiard 2.

These spectra have visual similarity with the wings of a butterfly. They possess the property of self-similarity (fractality) and are one of the not so numerous fractal structures discovered in quantum physics. Hofstadter's butterfly is a mathematical object with fractal structure describing the behavior of electrons in a magnetic field. Under the action of a magnetic field, free electrons move along circumferences.

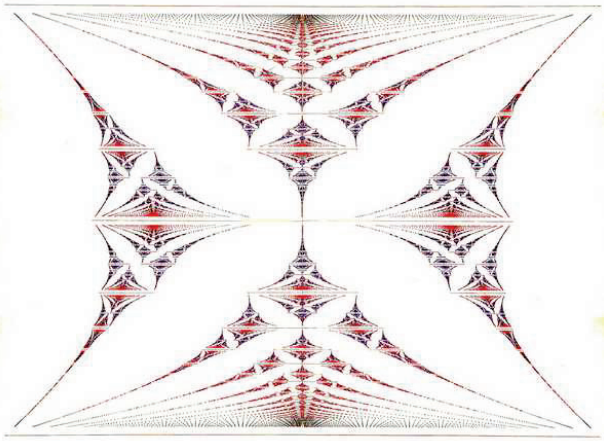

Fig. 9. This butterfly is a fractal describing the spectrum of electrons in a periodic structure with magnetic field.

The theory says that if the electrons are "locked" in a crystal atomic lattice, the trajectories of their motion will be much more complicated. An analogous situation is presented by the Andreev billiard. The fractal structures by themselves are rare in the quantum world. Therefore, Hofstadter's butterfly was not discovered for a long time, which was partially related to the complexity of experiments. Then scientists from Manchester succeeded to observe an intricate pattern on graphene in a magnetic field representing Hofstadter's butterfly.[17]

5. Conclusions

We have studied hybrid nanowires, in which normal and superconducting regions are in close proximity, by using the Bogoliubov–de Gennes equations for superconductivity in a cylindrical nanowire. We have developed a method for numerical solutions of these equations in FORTRAN program and present some preliminary results. We have succeeded to obtain the quantum energy levels and wavefunctions of a superconducting nanowire. The spectrum of states we calculated shows the interesting "Andreev billiard" characteristics. Preliminary results are also obtained in the cases of a magnetic nanowire and a superconducting nanowire containing a vortex. The calculations for a superconducting nanowire can be extended to the cases of a superconductor–ferromagnet hybrid nanowire and a nanowire containing one or more superconducting flux quanta.[12]

The obtained spectra of electrons remind Hofstadter's butterfly.[14]

Acknowledgments

We thank the JSPS for support through the JSPS Invitation Fellowship Program for Research in Japan No. S-15766.

References

1. A. Larkin and Y. Ovchinnikov, *Sov. Phys. J. Exp. Theoret. Phys.* **20**, 762 (1965).
2. P. Fulde and A. Ferrell, *Phys. Rev.* **135**, A550 (1964).
3. S. Kruchinin, H. Nagao and S. Aono, *Modern Aspects of Superconductivity: Theory of superconductivity* (World Scientific, Singapore, 2010), p. 220.
4. S. Kruchinin and H. Nagao, *Int. J. Mod. Phys. B* **26**, 1230013 (2012).
5. A. C. Mota *et al.*, *Physica B* **197**, 95 (1994).
6. F. B. Müller-Allinger, A. C. Mota and W. Belzig, *Phys. Rev. B* **59**, 8887 (1999).
7. F. B. Müller-Allinger and A. C. Mota, *Phys. Rev. Lett.* **84**, 3161 (2000).
8. F. B. Müller-Allinger and A. C. Mota, *Physica B* **284–288**, 683 (2000).
9. C. Caroli and J. Matricon, *Phys. Kondens. Mater.* **3**, 380 (1965).
10. I. F. Lyuksyutov and V. L. Pokrovsky, *Adv. Phys.* **54**, 67 (2005).
11. A. I. Buzdin, *Rev. Mod. Phys.* **77**, 935 (2005).
12. J. Wang *et al.*, *Nature Phys.* **6**, 389 (2010).
13. C. Portesi *et al.*, *J. Phys: Condens. Matter.* **20**, 474210 (2008).
14. D. Hofstadter, *Phys. Rev. B* **14**, 2239 (1976).
15. F. Gygi and M. Schlüter, *Phys. Rev. B* **43**, 7609 (1991).
16. A. A. Shanenko *et al.*, in *Proc. of NATO-ARW: Physical Properties of Nanosystems*, eds. J. Bonca and S. Kruchinin (Springer, Berlin, 2008), pp. 340–348.
17. A. V. Kretinin *et al.*, *Nano Lett.* **14**(6), 3270 (2014).